

Extended one-dimensional Hubbard model: A small-cluster approach

L. Milans del Bosch

Departamento de Física de la Materia Condensada, Universidad Autónoma de Madrid, 28049 Madrid, Spain

L. M. Falicov*

NORDITA, Blegdamsvej 17, DK-2100 Copenhagen Ø, Denmark

and Materials and Chemical Sciences Division, Lawrence Berkeley Laboratory, Berkeley, California 94720

(Received 25 August 1987)

The one-dimensional Hubbard model with nearest-neighbor hopping, first- and second-nearest-neighbor particle interactions, and one particle per site is reexamined by means of a small-crystal approach—an exact solution of a four-site cluster with periodic boundary conditions. Lines of symmetry crossing as well as singular lines and points are found. Analysis of correlation functions indicates that although there are smooth, strong changes as the parameters approach the values of the charge-to-spin-density-wave transition (a suggestion of an incipient second-order transition), the actual change involves a crossover between unrelated symmetries (a clear indication of a first-order transition). The relatively simple calculation and its results agree well with previous Monte Carlo numerical simulations and settles the unresolved question of the order of the density-wave transition.

I. INTRODUCTION

Since its introduction in 1963, the Hubbard model¹ has become the prototype of a system of fermions with short-range interactions. It has been used to study a great variety of many-body effects in metals, of which ferromagnetism, antiferromagnetism, metal-insulator transitions, spin-density waves, charge-density waves, and superconductivity are the most common examples.^{1–7}

The model has been applied to a variety of lattices—one, two, and three dimensional^{2,3,8–12}—and to small clusters.^{13–17} Exact solutions are available for one dimension⁸ and for small clusters,^{13–17} and exact theorems have been proved for some cases.¹⁸ Since the numerical solution of extended cases is in general very laborious and computationally expensive,⁹ exact results easily obtainable with relatively small clusters with periodic boundary conditions^{13–17} are an appealing alternative for studying these complex systems. It should be remembered that a cluster of N sites with periodic boundary conditions—the so-called small-crystal approach—is exactly equivalent to an extended periodic system in which the sampling of the Brillouin zone is restricted to N specific points.^{19–22}

It is the object of this contribution to examine once again the extended one-dimensional Hubbard model^{9–11} by means of the small-crystal approach. The model consists of a one-dimensional chain, with one fully symmetric orbital per site, an occupancy of one electron per site, one-electron hopping of strength $-t$ between nearest-neighbor sites, and two-electron interactions between electrons in the same site (U), and between electrons in neighboring sites (K). The system is known to exhibit symmetry transitions in its ground state as a function of the parameters. The transitions have been found in weak-coupling^{23,24} and strong-coupling²⁵ theories, with

real-space scaling methods,^{10,11} as well as in Monte Carlo simulations.⁹ There seems to be a controversy over the order and nature of these transitions, which our calculation can definitely help to clarify. Section II contains the definition of the problem, the method of solution and the details of the calculation. Section III presents the results and conclusions.

II. MODEL AND METHOD OF CALCULATION

The one-dimensional extended Hubbard model consists of a very large (infinite) chain of sites i separated by a distance a and with periodic-boundary conditions. There is one s orbital per site, each being either spin up or down, denoted with subscript σ . The electron creation (destruction) operator is written as $c_{i\sigma}^\dagger$ ($c_{i\sigma}$). The Hamiltonian consists of three terms:

$$H = H_{\text{band}} + H_{\text{intra}} + H_{\text{neighbor}}, \quad (2.1)$$

where

$$H_{\text{band}} = -t \sum_{i,\sigma} (c_{i\sigma}^\dagger c_{i+1,\sigma} + c_{i\sigma}^\dagger c_{i-1,\sigma}), \quad (2.2)$$

$$H_{\text{intra}} = U \sum_i c_{i\uparrow}^\dagger c_{i\uparrow} c_{i\downarrow}^\dagger c_{i\downarrow}, \quad (2.3)$$

$$H_{\text{neighbor}} = K \sum_{i;\sigma,\sigma'} c_{i\sigma}^\dagger c_{i\sigma} c_{i+1,\sigma'}^\dagger c_{i+1,\sigma'}. \quad (2.4)$$

These terms are the following (a) a band “hopping” interaction (2.2) between electron states on adjacent sites, with transfer integral $-t$; (b) an on-site (intra-atomic) interaction (2.3) of strength U ; and (c) a nearest-neighbor (inter-atomic) interaction (2.4) of strength K . Only an

average occupancy of one electron per site is considered in this contribution but, for the sake of completeness, cases of U and K of either sign are considered.

The system has one-dimensional translational invariance, and consequently a Brillouin zone which extends over the interval

$$-\pi/a < k \leq \pi/a .$$

In particular we identify the following points in the zone,

$$k = 0, \text{ point } \Gamma , \quad (2.5)$$

$$k = \pi/a, \text{ point } X , \quad (2.6)$$

$$k = \pm\pi/2a, \text{ point } A, A' . \quad (2.7)$$

If the four points in k space mentioned above are the only ones selected to sample the Brillouin zone, the problem is then reduced to the solution of a cluster of four atoms, in linear arrangement and with periodic-boundary conditions. The cluster contains all together four electrons. Group-theoretical analysis of the cluster symmetry and physical properties yields nine possible symmetries, corresponding to space representations Γ , X , and A , and total spin $S=0$ (spin singlets), $S=1$ (spin triplets), and $S=2$ (spin quintets). The degeneracies of these representations are shown in Table I.

The cluster has $8!/4!4! = 70$ states arranged in no more than 28 symmetry-required energy levels. The distribution of those levels among the nine possible symmetries is shown in Table II. It should be emphasized that these levels are dictated by the symmetry of the problem, and that many times the Hubbard model, for general interactions, shows additional (accidental) degeneracies, i.e., the number of levels for this cluster may be, in general, less than 28. For specific values of the parameters the degeneracy is indeed greater. In particular for $U=K=0$, the noninteracting particle limit, the number of levels reduces to five (see Table III). In the extreme strong-interaction limit, $t=0$, there are also five levels (see Table IV), with further reductions in very special cases (e.g., $U=K$, $U=0$, and $K=0$).

An analysis of the limits²³⁻²⁵ is easy and instructive.

(A) The noninteracting limit, $U=K=0$, shows a sixfold degenerate ground state of energy $(-4t)$ and symmetries $^3\Gamma$, $^1\Gamma$, and 1X .

The strongly interacting limit is more interesting and complex. The results of its analysis depend on whether the number of electrons is strictly restricted to four in the four-site cluster, or whether number fluctuations are allowed. (B) For $t=0$ and the number of electrons strictly restricted to four in the cluster the results are as follows: (B1) For $U < 0$, $K < 0$ the ground state is fourfold degenerate, its energy is $2U + 4K$, and the contributing sym-

metries are $^1\Gamma$, 1X , and 1A . The corresponding distribution of electrons is $(\dots 2200220022 \dots)$, in which the electrons tend to cluster together to take full advantage of the nearest-neighbor and second-neighbor attractive interactions; (B2) For $U > 0$, $K < U/2$ the ground state is sixteenfold degenerate, its energy is $4K$, and the contributing symmetries are $^1\Gamma$, 1X , 3X , 3A , and 5X . The electron distribution corresponds to $(\dots 1111111111 \dots)$ and arbitrary spin orientations, which include ferromagnetism (the spin quartet), ferrimagnetism (the spin triplets) and spin-density waves (the spin singlets); (B3) For $K > 0$, $U < 2K$ the ground state is twofold degenerate, its energy is $2U$, and the contributing symmetries are $^1\Gamma$ and 1X . The electron distribution corresponds to $(\dots 20202020 \dots)$, i.e., charge-density waves.

(C) If, on the other hand, only the average number of electrons is restricted to four per cluster, and fluctuations are allowed, the results get considerably modified: (C1) For $K < 0$, $U < (-2K)$ the state of minimum energy is a heterogeneous admixture of equal amounts of two phases, one with eight electrons per cluster [full cluster with electron distribution $(\dots 2222222222 \dots)$] and symmetry $^1\Gamma$, the other with no electrons [empty cluster with electron distribution $(\dots 0000000000 \dots)$] and also of symmetry $^1\Gamma$. The average energy of this two-phase composite is $2U + 8K$; (C2) The structures described in (B2) are still stable, but only for $U > 0$, $-U/2 < K < U/2$; (C3) The structures described in (B3) and their boundaries remain unchanged.

The conclusions to be drawn from (A), (B), and (C) are the following: (i) since the symmetries $^1\Gamma$ and 1X contribute to the ground-state manifold in all limits of (A) and (B) it is likely that, for any of the values of the parameters t , U , and K , the ground state will be either $^1\Gamma$, or 1X ; (ii) the heterogeneous admixture described in (C1) comprises only empty and full bands, and is therefore independent of the band term (2.2), i.e., its energy is $2U + 8K$ and will remain stable as long as that energy is the absolute minimum; (iii) there must be phase transitions, either of first or of higher order, in the three limits

$$U = 2K \rightarrow +\infty ,$$

$$U = -2K \rightarrow +\infty ,$$

$$K = 0, \quad U \rightarrow -\infty .$$

It is always possible that additional phase transitions exist in other regions of parameter space.

The symmetries $^1\Gamma$ and 1X have been completely analyzed in the four-site cluster. As shown in Table II each of these symmetries involves the diagonalization of a sim-

TABLE I. Degeneracy of the various representations.

	Γ	X	A
$S=0$	1	1	2
$S=1$	3	3	6
$S=2$	5	5	10

TABLE II. Multiplicity of the matrices for the various representations.

	Γ	X	A
$S=0$	6	6	4
$S=1$	4	3	4
$S=2$	0	1	0

TABLE III. The 28 energy levels in the limit $U=K=0$.

E	Degeneracy	${}^3\Gamma$	${}^1\Gamma$	5X	3X	1X	3A	1A
$-4t$	6	1	1	0	0	2	0	0
$-2t$	16	0	0	0	0	0	2	2
0	26	2	4	1	3	2	0	0
$2t$	16	0	0	0	0	0	2	2
$4t$	6	1	1	0	0	2	0	0

TABLE IV. The 28 energy levels in the limit $t=0$.

E	Degeneracy	${}^3\Gamma$	${}^1\Gamma$	5X	3X	1X	3A	1A
$4K$	16	1	1	1	0	1	1	0
$U+3K$	32	2	2	0	2	2	2	2
$U+4K$	16	1	1	0	1	1	1	1
$2U+4K$	4	0	1	0	0	1	0	1
$2U$	2	0	1	0	0	1	0	0

TABLE V. Hamiltonian matrix for the ${}^1\Gamma$ symmetry.

$2U$	$-2t\sqrt{2}$	0	0	0	0
$-2t\sqrt{2}$	$U+3K$	$-2t\sqrt{2}$	0	0	0
0	$-2t\sqrt{2}$	$U+4K$	U	0	0
0	0	U	$U+4K$	0	0
0	0	0	0	$U+4K$	0
0	0	0	0	0	$U+3K$

TABLE VI. Hamiltonian matrix for the 1X symmetry.

$2U$	$2t\sqrt{2}$	0	0	0	0
$2t\sqrt{2}$	$U+3K$	$2t\sqrt{2}$	0	0	0
0	$2t\sqrt{2}$	$U+4K$	0	0	0
0	0	0	$4K$	$-2t\sqrt{3}$	0
0	0	0	$-2t\sqrt{3}$	$U+3K$	$2t$
0	0	0	0	$2t$	$2U+4K$

TABLE VII. Expectation values of the correlation operators for limiting cases.

State	O_{CNN}	O_{CSN}	O_{SNN}	O_{SSN}
2020	1	0	0	0
2200	$\frac{1}{2}$	1	0	0
$\uparrow\uparrow\uparrow\uparrow$	0	0	0	0
$\uparrow\downarrow\uparrow\downarrow$	0	0	1	0
$\uparrow\uparrow\downarrow\downarrow$	0	0	$\frac{1}{2}$	1

ple 6×6 matrix. The two matrices were generated by standard group-theoretical techniques and are shown in Tables V and VI.

Diagonalization of these matrices yields eigenvalues and eigenfunctions which contain the required information. Results of the diagonalization are presented in the next section.

In order to study thoroughly the nature of the ground state and to obtain useful information about the nature of the transitions, four correlation operators are defined, and their expectation values calculated for the ground-state wave function,

$$\alpha = \langle \psi | O_\alpha | \psi \rangle, \quad (2.8)$$

where ψ stands for the ground-state eigenvector, and α takes four values (1) α_{CNN} corresponding to charge, nearest-neighbor correlations, (2) α_{CSN} corresponding to charge, second-nearest-neighbor correlations, (3) α_{SNN} corresponding to spin, nearest-neighbor correlations, and (4) α_{SSN} corresponding to spin, second-nearest-neighbor correlations. The operators O_α are given in the Appendix. It should be noted that these correlation functions are positive-definite quantities which vary between 0 and 1. Discontinuities in these coefficients as functions of the parameters correspond to level crossings and are strong indications of a first-order phase transition in the system. Rapid but continuous changes in the α 's are a strong indication of higher-order phase transitions. Table VII gives the values of the four α 's for five limiting cases.

III. RESULTS AND CONCLUSIONS

Figure 1 shows the division of parameter space (U/t)-(K/t) according to symmetry of the ground state. There are three-regions, (i) a homogeneous region of symmetry $^1\Gamma$ (the charge-density-wave region); (ii) a homogeneous region of symmetry 1X (the spin-density-wave region); and (iii) a heterogeneous region of phase separation between the full, charged (eight electrons) and the fully empty (no electrons) clusters. These regions are separated by two first-order lines corresponding *exactly* to $U=2K$ and to $E=2U+8K$. They intersect at a singular point in the diagram

$$\begin{aligned} (U/t) &= -\left(\frac{10}{7}\right)^{1/2}, \\ (K/t) &= -\left(\frac{5}{14}\right)^{1/2}, \\ (E/t) &= -\left(\frac{360}{7}\right)^{1/2}. \end{aligned} \quad (3.1)$$

There is also a singular line $U=0, K>0$, where the ground state is accidentally degenerate, with symmetries $^1\Gamma$ and 1X coalescing there. The noninteracting case ($U=K=0$) is also a very singular point where, as said before, six states and three symmetry levels $^3\Gamma$, $^1\Gamma$, and 1X become degenerate.

It should be remarked that, as discussed in the previous section, both the spin-density-wave and the charge-density-wave states admit both symmetries: $^1\Gamma$ and 1X . The fact that the minimum energy is achieved by different representations in each case is a strong indica-

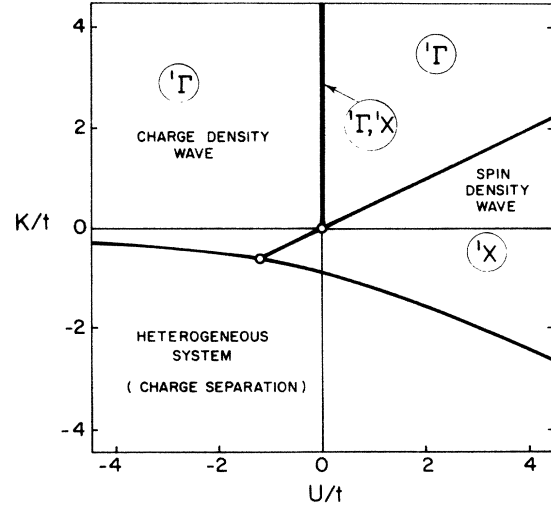


FIG. 1. The $T=0$ phase diagram as a function of U/t and K/t . There is a line of discontinuities separating the $^1\Gamma$ and the 1X symmetries and a second line of discontinuities separating either phase from the heterogeneous admixture of the charge-separated phases. The line $U=0, K>0$ has an accidentally degenerate ground state. There are also two singular points in the diagram: $U=K=0$ (the noninteracting case) and $U=2K=-1.1952t$, where the two lines of discontinuity meet.

tion that the phase transition should involve an "unrelated" symmetry change, i.e., be of the first-order type.

Ground-state energies are shown in Fig. 2. Figures 3–6 show the four α correlation functions defined in the preceding section and in the Appendix. An analysis of these figures yields the following conclusions: (i) all correlation functions are discontinuous along the line of charge separation, $E=2U+8K$; (ii) the nearest-neighbor correlation functions α_{CNN} and α_{SNN} are discontinuous along the $U=2K$ line; (iii) the second-nearest-neighbor

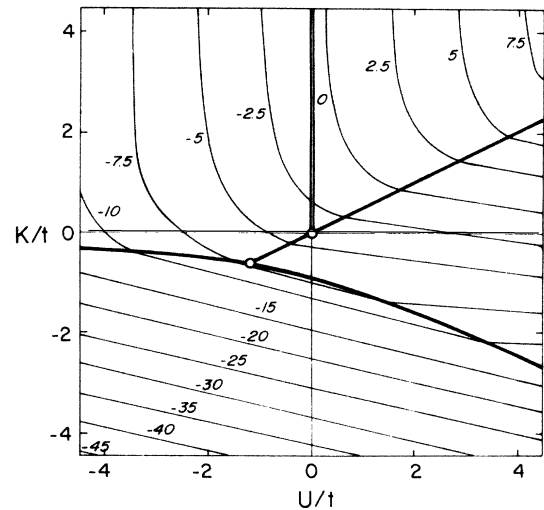


FIG. 2. The ground-state energy, in units of t , as a function of U/t and K/t . The energy takes the value $-4t$ for $U=K=0$ and the value $-7.1714t$ for $U=2K=-1.1952t$ (the two singular points).

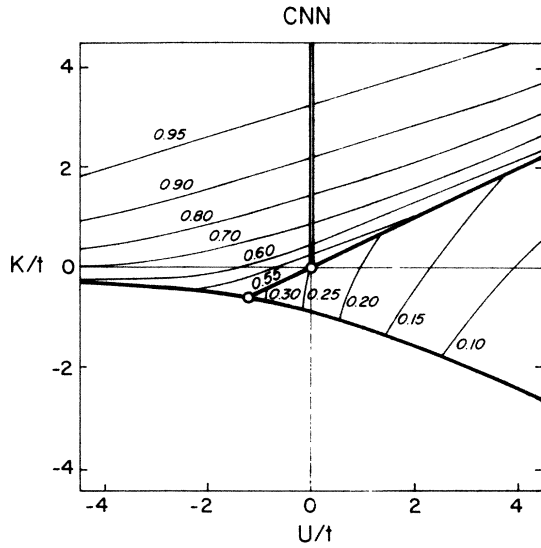


FIG. 3. The correlation function α_{CNN} for charge, nearest neighbors, as a function of U/t and K/t . Note the discontinuity of the function along the $U=2K$ line, and the strong correlation in the $^1\Gamma$ ground-state region.

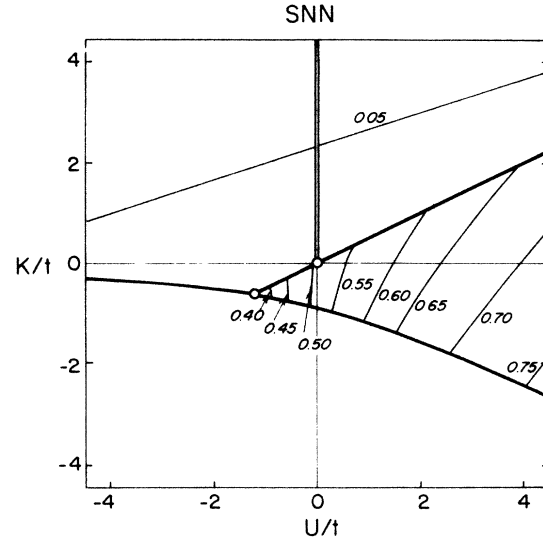


FIG. 5. The correlation function α_{SNN} for spin, nearest neighbors, as a function of U/t and K/t . Note the discontinuity of the function along the $U=2K$ line and the strong correlation in the 1X ground-state region.

correlation functions α_{CSN} and α_{SSN} are continuous along the same line, but exhibit slope discontinuities (kinks) there; (iv) α_{CNN} is large in the charge-density-wave region (indicating nearest-neighbor charge oscillations), and small elsewhere; (v) α_{SNN} is large in the spin-density-wave region (indicating nearest-neighbor spin oscillations), and small elsewhere; (vi) α_{CSN} is small everywhere, except in the region of large negative values of both U and K , close to the line of charge separation; (vii) α_{SSN} is small throughout; (viii) α_{CNN} , near the $U=2K$ line and in the charge-density-wave region, has a rapid decrease indica-

tive of an incipient “higher-order” transition to the $^1\Gamma$ spin-density-wave state; however, exactly at the $U=2K$ line there is a symmetry crossover and the 1X symmetry becomes the spin-density-wave ground state; (ix) the first-order charge- to spin-density-wave transition is *exactly* at the $U=2K$ line and not, as found in Monte Carlo calculations,⁹ at values of U slightly smaller than $2K$; the discrepancy may be caused by the small cluster approach, but it may also be due to the strong “second-order” precursor on the charge-density-wave side, which may (in the numerical simulations) spuriously displace the transi-

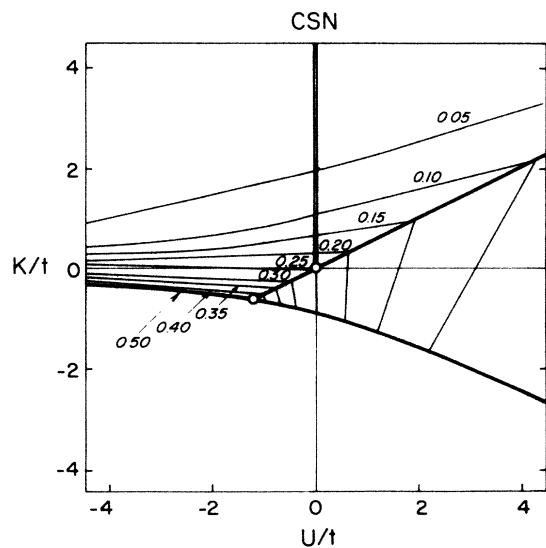


FIG. 4. The correlation function α_{CSN} for charge, second-nearest neighbors, as a function of U/t and K/t . Note that the function is continuous along the $U=2K$ line, but exhibits slope discontinuities (kinks) there; there is strong anticorrelation almost everywhere in the diagram.

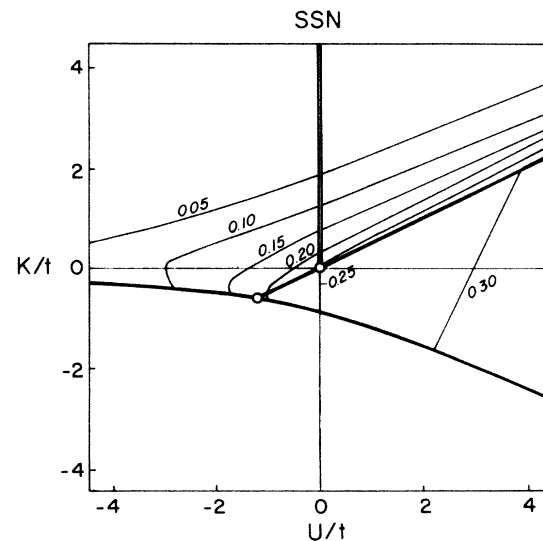


FIG. 6. The correlation function α_{SSN} for spin, second-nearest neighbors, as a function of U/t and K/t . Note that the function is continuous along the $U=2K$ line, but exhibits slope discontinuities (kinks) there; there is strong anticorrelation everywhere in the diagram.

tion away from $U=2K$, as well as yield a second-order transition for $U \sim 2K \sim 0$; (x) in the vicinity of the line of degeneracy, $U=0$, $K>0$, where the ground state is accidentally degenerate, there must be complicated finite-temperature effects, and therefore equally complex numerical simulation results, which may be the cause for the discrepancies between previously published results.

In conclusion, the exact solution of a half-filled, four-site cluster extended Hubbard model, with periodic-boundary conditions indicates once again that simple models are surprisingly rich in structure, that symmetry crossovers are common, and that numerical simulations and perturbation expansions should be handled with extreme care and an unusually critical eye.

APPENDIX

The four operators used in the text to calculate ground-state correlation functions are defined in what follows. The four atoms in the cluster are numbered $i=0, 1, 2$, and 3 , where 0 and 2 and 1 and 3 are the two second-nearest-neighbor pairs. The number operators are

$$n_{i\sigma} \equiv c_{i\sigma}^\dagger c_{i\sigma}. \quad (\text{A1})$$

If the following five two-particle operators are defined,

$$P(0;a) \equiv \frac{1}{2}(n_{0\uparrow}n_{0\downarrow} + n_{1\uparrow}n_{1\downarrow} + n_{2\uparrow}n_{2\downarrow} + n_{3\uparrow}n_{3\downarrow}), \quad (\text{A2})$$

$$P(1;p) \equiv \frac{1}{4}(n_{0\uparrow}n_{1\uparrow} + n_{0\downarrow}n_{1\downarrow} + n_{1\uparrow}n_{2\uparrow} + n_{1\downarrow}n_{2\downarrow} + n_{2\uparrow}n_{3\uparrow} + n_{2\downarrow}n_{3\downarrow} + n_{3\uparrow}n_{0\uparrow} + n_{3\downarrow}n_{0\downarrow}), \quad (\text{A3})$$

$$P(1;a) \equiv \frac{1}{4}(n_{0\uparrow}n_{1\downarrow} + n_{0\downarrow}n_{1\uparrow} + n_{1\uparrow}n_{2\downarrow} + n_{1\downarrow}n_{2\uparrow} + n_{2\uparrow}n_{3\downarrow} + n_{2\downarrow}n_{3\uparrow} + n_{3\uparrow}n_{0\downarrow} + n_{3\downarrow}n_{0\uparrow}), \quad (\text{A4})$$

$$P(2;p) \equiv \frac{1}{2}(n_{0\uparrow}n_{2\uparrow} + n_{0\downarrow}n_{2\downarrow} + n_{1\uparrow}n_{3\uparrow} + n_{1\downarrow}n_{3\downarrow}), \quad (\text{A5})$$

$$P(2;a) \equiv \frac{1}{2}(n_{0\uparrow}n_{2\downarrow} + n_{1\uparrow}n_{3\downarrow} + n_{2\uparrow}n_{0\downarrow} + n_{3\uparrow}n_{1\downarrow}), \quad (\text{A6})$$

then the required correlation operators are

$$O_{\text{CNN}} = \frac{1}{2}[1 + P(0;a) - P(1;p) - P(1;a)], \quad (\text{A7})$$

$$O_{\text{CSN}} = \frac{1}{2}[1 + P(0;a) - P(2;p) - P(2;a)], \quad (\text{A8})$$

$$O_{\text{SNN}} = \frac{1}{2}[1 - P(0;a) - P(1;p) + P(1;a)], \quad (\text{A9})$$

$$O_{\text{SSN}} = \frac{1}{2}[1 - P(0;a) - P(2;p) + P(2;a)]. \quad (\text{A10})$$

Expectation values of these operators can be between 0 and 1. Values greater than $\frac{1}{2}$ indicate positive correlation, i.e., charge (C) or spin (S) oscillations. Values smaller than $\frac{1}{2}$ indicate tendency towards charge (C) or spin (S) uniformity for that particular site separation (NN for nearest neighbors, SN for second-nearest neighbors). Expectation values of these operators for limiting cases are shown in Table VII.

ACKNOWLEDGMENTS

The authors want to thank Professor Félix Yndurain for stimulating and illuminating discussions. L.M.F. would like to acknowledge the hospitality of the Universidad Autónoma de Madrid in Spain, where this research was started, and of the Nordisk Institut for Teoretisk Atomfysik (NORDITA) and the H. C. Ørsted Institutet in Copenhagen, where he completed the last stages of the investigation. This research was supported in Spain by Comisión Asesora Interministerial de Ciencia y Tecnología and at the Lawrence Berkeley Laboratory by the Director, Office of Energy Research, Office of Basic Energy Sciences, Materials Science Division, U.S. Department of Energy, under Contract No. DE-AC03-76SF00098.

*Permanent address: Department of Physics, University of California, Berkeley, CA 94720.

¹J. Hubbard, Proc. R. Soc. London, Ser. A **276**, 238 (1963); **277**, 237 (1964); **281**, 401 (1964); **285**, 542 (1965); **296**, 82 (1966); **296**, 100 (1967).

²D. R. Penn, Phys. Rev. **142**, 350 (1966).

³D. Denley and L. M. Falicov, Phys. Rev. B **17**, 1289 (1978).

⁴D. Adler, in *Solid State Physics*, edited by H. Ehrenreich, F. Seitz, and D. Turnbull (Academic, New York, 1968), Vol. 21, p. 1.

⁵Proceedings of the International Conference on Metal-Nonmetal Transitions, San Francisco, 1968 [Rev. Mod. Phys. **40**, 673 (1968)].

⁶N. F. Mott and G. Zinamon, Rep. Prog. Phys. **33**, 881 (1970).

⁷P. W. Anderson, Science **235**, 1196 (1987).

⁸E. H. Lieb and F. Y. Wu, Phys. Rev. Lett. **20**, 1145 (1968).

⁹J. E. Hirsch, Phys. Rev. Lett. **53**, 2327 (1984).

¹⁰B. Fourcade and G. Spronken, Phys. Rev. B **29**, 5089 (1984).

¹¹B. Fourcade and G. Spronken, Phys. Rev. B **29**, 5096 (1984).

¹²K. B. Whaley and L. M. Falicov, J. Chem. Phys. **87**, 7160 (1987).

¹³L. M. Falicov and R. A. Harris, J. Chem. Phys. **51**, 3153 (1969).

¹⁴L. M. Falicov and R. H. Victora, Phys. Rev. B **30**, 1695 (1986).

¹⁵J. Callaway, D. P. Chen, and Y. Zhang, Z. Phys. D **3**, 91 (1986).

¹⁶J. Callaway, D. P. Chen, and Y. Zhang, Phys. Rev. B **35**, 3705 (1987).

¹⁷J. Callaway, D. P. Chen, and Y. Zhang (private communication).

¹⁸E. H. Lieb and D. Mattis, Phys. Rev. **125**, 164 (1962).

¹⁹R. H. Victora and L. M. Falicov, Phys. Rev. Lett. **55**, 1140 (1985).

²⁰E. C. Sowa and L. M. Falicov, Phys. Rev. B **35**, 3765 (1987).

²¹A. Reich and L. M. Falicov, Phys. Rev. B **34**, 6752 (1986).

²²A. Reich and L. M. Falicov, Phys. Rev. B **36**, 3117 (1987).

²³J. Solyom, Adv. Phys. **21**, 201 (1979).

²⁴V. J. Emery, in *Highly Conducting One-Dimensional Solids*, edited by J. Devreese, R. Evrand, and V. van Doren (Plenum, New York, 1979).

²⁵R. A. Bari, Phys. Rev. B **3**, 2662 (1971).